A Study of Brownian Motion Using Light Scattering*,†

NOEL A. CLARK, JOSEPH H. LUNACEK, AND GEORGE B. BENEDEK
Center for Materials Science and Engineering and Physics Department, Massachusetts Institute of Technology, Cambridge, Massachusetts 02139

(Received 4 December 1969)

From the spectrum of light scattered by a suspension of particles in a fluid one can obtain quantitative information about the motion of the particles, including an accurate determination of their diffusion constant. If the incident light source is a laser, and the scattered light falls on the photosurface of a photomultiplier tube, then by measuring the spectrum of the photocurrent one obtains the spectrum of the intensity fluctuations of the scattered light. The intensity of the scattered light is determined by the instantaneous superposition of the phases of the waves scattered from each of the diffusing particles and the intensity fluctuates because the particles move. For particles of known diameter one can predict the spectral shape and width from the diffusion equation. We present a calculation of the spectrum of the field and the spectrum of the intensity of the scattered light and an advanced laboratory experiment and lecture demonstration by which the intensity spectrum can be studied.

I. INTRODUCTION

It has been demonstrated theoretically[1] and experimentally[2,3] that the diffusive motion of a system of particles may be investigated by studying the very narrow spectrum of the initially monochromatic light scattered by the particles. A number of review papers describing this type of investigation are now becoming available.[4,5] Specifically, the frequency spectrum of the scattered light provides the conditional probability $[P(\mathbf{r}, t \mid 0, 0)d^3r]$ that a particle originally located at $\mathbf{r}=0$ and $t=0$ will be found within a volume d^3r around $\mathbf{r}$ some time t later. If a particle undergoes a random walk or Brownian motion, the form of $P(\mathbf{r}, t \mid 0, 0)$ is well known and is given by[6]

$$P(\mathbf{r}, t \mid 0, 0) = (4\pi Dt)^{-3/2} \exp(-r^2/4Dt) \quad (1)$$

when the distance $\mathbf{r}$ contains many steps in the random walk.

The temporal evolution of $P(\mathbf{r}, t \mid 0, 0)$ is determined by the diffusion constant D for the wandering particle. If the particle is a sphere whose diameter $(2a)$ is large compared to molecular dimensions, the Stokes–Einstein relation connects the diffusion constant to the viscosity η of the solvent and the temperature T by the equation[7]

$$D = k_B T/6\pi\eta a, \quad (2)$$

where k_B is Boltzmann's constant. The spectral shape of the scattered light enables an experimental verification of the form of $P(\mathbf{r}, t \mid 0, 0)$ and a determination of D, the diffusion constant.

The experimental arrangement is shown in Fig. 1. Light from a helium–neon laser producing at least 1 mW of power is focused onto a cell containing a dilute aqueous solution of monodisperse (uniform diameter) polystyrene spheres. Each illuminated particle will scatter light that falls on it because its index of refraction is different from that of the surrounding water. The light scattered into a small range of angles about some angle Θ is

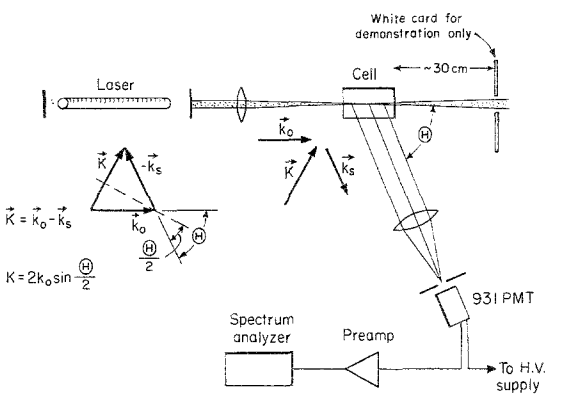

FIG. 1. Block diagram of experimental apparatus. The laser output is polarized normal to the scattering plane and focused in the cell (1×2×5 cm) by a lens of focal length 8 cm. The collecting lens has a focal length of about 20 cm. Vectors $\mathbf{k}_0$ and $\mathbf{k}_s$ represent the incident and scattered wave vectors, respectively.

collected onto the photosurface of an RCA 931 photomultiplier tube (PMT). The photomultiplier output current is proportional to the *intensity* of the light falling on the photocathode. This intensity, however, is constantly fluctuating around its average value because the phase of the field scattered by each particle relative to that of

the other particles changes in time as the particles move. The temporal fluctuations in the photocurrent output are thus a measure of the random walking of the particles. In the following section, we shall show quantitatively how the spectrum of the scattered light and the spectrum of the photocurrent reflects the random motion of the scattering particles. We anticipate here the final result. If the particles move independently of one another, and if the conditional probability for the motion of each is given by Eq. (1), then the frequency spectrum $S_I(\omega)$ of the intensity of the scattered light (and hence the frequency spectrum of the photocurrent) will have the form of a Lorentzian shaped line whose width Γ depends on D and on the scattering angle Θ as follows:

$$S_I(\omega) \propto \Gamma(\Theta)/[\omega^2+\Gamma^2(\Theta)], \tag{3}$$

where

$$\omega = 2\pi f, \tag{4}$$

$$\Gamma(\Theta) = 2D\left(\frac{4\pi}{\lambda/n}\sin\tfrac{1}{2}\Theta\right)^2. \tag{5}$$

Here λ is the wavelength of the incident light, n is the index of refraction of the solution, and Θ is the scattering angle.

It is important to point out that the frequency spectrum of the scattered electric field, as contrasted with the frequency spectrum of the scattered *intensity*, is also a Lorentzian line, but its center is located at the incident light frequency which is $\sim 10^{14}$ Hz. Since the spectral width of the scattered field is ~ 500 Hz, measurement of its width would be quite impossible because no filters of such narrow width are available in the optical-frequency region. The spectrum of the intensity of the light is twice as broad as that of the electric field but is centered at zero frequency. Here narrow-band electrical filters can easily be obtained to measure the spectral distribution in the photocurrent and hence the spectrum of the intensity of the light. This in turn permits determination of the diffusion constant of the particles.

II. CALCULATION OF THE SPECTRUM OF THE SCATTERED ELECTRIC FIELD AND THE SPECTRUM OF THE SCATTERED LIGHT INTENSITY

Let a plane wave of the form $\mathbf{E}_0\exp[i(\mathbf{k}_0\cdot\mathbf{r}-\omega_0 t)]$ illuminate the solution of particles. Here $\mathbf{k}_0$ is the wave vector of the incident light beam and ω_0 is the angular frequency of the wave. This field induces in each of the particles a radiating dipole moment. The total electric field $\mathbf{E}(t)$ at a detector a distance $\mathbf{R}$ from some origin within the region of illumination is the sum of the fields radiated by each of the particles, and has the form

$$\mathbf{E}(t) = \sum_{j=1}^{N}\mathbf{E}_j(t) = \sum_{j=1}^{N}\mathbf{E}_0'\exp[i\phi_j(t)-i\omega_0 t]. \tag{6}$$

Here E_0' is the amplitude of the field scattered by each of the particles and is independent of the position of the particle. It is given by

$$E_0' = E_0[\exp(i\mathbf{k}_s\cdot\mathbf{R})/R](\omega/c)^2(\alpha-\alpha_0)V\sin\Phi, \tag{7}$$

where $\mathbf{k}_s$ is the wave vector of the scattered wave, Φ is the angle between the direction of polarization of $\mathbf{E}_0$ and the direction $\mathbf{k}_s$ of propagation of the scattered wave, $\alpha-\alpha_0$ is the difference between the dipole polarizability of the particle and the solvent, and V is the volume of the scattering particle. The precise position of the jth particle enters through the phase factor $\phi_j(t)$. This phase is $2\pi/\lambda$ (where λ is the wavelength of the light) times the difference in path length between the particle (j) and a point at the origin 0, as is indicated in Fig. 2. Thus

$$\phi_j(t) = (2\pi/\lambda)(\bar{C}\bar{P}\bar{D}-\bar{A}\bar{O}\bar{B}) = \mathbf{k}_0\cdot\mathbf{r}_j-\mathbf{k}_s\cdot\mathbf{r}_j \tag{8}$$

$$\phi_j(t) = (\mathbf{k}_0-\mathbf{k}_s)\cdot\mathbf{r}_j(t). \tag{9}$$

We may conveniently define a scattering vector $\mathbf{K}$ as the difference between the incident and scattered wave vectors (see Fig. 1):

$$\mathbf{K} = \mathbf{k}_0-\mathbf{k}_s. \tag{10}$$

The magnitude of this scattering vector is given by

$$K = 2k_0\sin\tfrac{1}{2}\Theta = \frac{4\pi}{\lambda/n}\sin\tfrac{1}{2}\Theta, \tag{11}$$

where Θ, the scattering angle, is the angle between $\mathbf{k}_0$ and $\mathbf{k}_s$, and n is the index of refraction of the medium. In terms of the scattering vector $\mathbf{K}$, $\phi_j(t)$ is given by

$$\phi_j(t) = \mathbf{K}\cdot\mathbf{r}_j(t). \tag{12}$$

We observe that the phase of the scattering particle changes only if it moves along the direction of $\mathbf{K}$. Motion normal to $\mathbf{K}$ does not alter the phase of the scattered wave. The phase $\phi_j(t)$ changes by 2π when the particle moves a distance $\Delta r_j = 2\pi/K$ along the direction of $\mathbf{K}$.

Both the scattered electric field $\mathbf{E}(t)$ and the intensity of the scattered light $I(t)=\beta\,|\,E(t)|^2$ are random variables because the phase of the wave scattered by each particle varies randomly in time as the particle diffuses from point to point. It is impossible to predict the detailed temporal variation of $\mathbf{E}(t)$ or of $I(t)$. In fact such information is not necessary. The quantities needed to characterize such a random variable are those like $\langle I(t)\rangle$, the average intensity, and $\langle I(t)I(t+\tau)\rangle$ and $\langle \mathbf{E}^*(t)\mathbf{E}(t+\tau)\rangle$; the correlation functions for the intensity and the field, respectively. The intensity correlation function is formed by measuring $I(t)$ and $I(t+\tau)$ for many similarly prepared systems and ensemble averaging their product. If the temporal fluctuations in $I(t)$ are "stationary" then $\langle I(t)I(t+\tau)\rangle$ is independent of starting time t and depends only on the difference τ. The spectrum of such a random process is intimately related to its correlation function. The Wiener–Khintchine theorem[8] provides this relationship. Thus, if $R_E(\tau)=\langle \mathbf{E}^*(t)\mathbf{E}(t+\tau)\rangle$ and $R_I(\tau)=\langle I(t)I(t+\tau)\rangle$, then the spectrum $S_E(\omega)$ of the scattered field and the spectrum $S_I(\omega)$ of the scattered intensity are given by

$$S_E(\omega)=\int_{-\infty}^{\infty} e^{i\omega\tau}R_E(\tau)\,d\tau \tag{13}$$

and

$$S_I(\omega)=\int_{-\infty}^{\infty} e^{i\omega\tau}R_I(\tau)\,dt. \tag{14}$$

The spectrum of the electric field as given in Eq. (13) is what one would obtain from a conventional optical spectrometer such as a diffraction grating or a Fabry–Perot interferometer. The spectrum of the *intensity fluctuations* $S_I(\omega)$ as given in Eq. (14) is proportional to the spectrum of the photocurrent fluctuations that are produced in the anode of a phototube when the cathode is illuminated with the scattered light. The photocurrent is proportional in part to the intensity of the incident light.

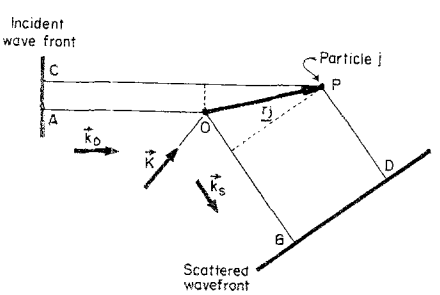

FIG. 2. Geometry for calculation of the phase of light scattered from particle j. The path length from an incident to a scattered wave front is $\bar{C}\bar{P}\bar{D}$ for light scattered by particle j and $\bar{A}\bar{O}\bar{B}$ for a particle at the origin 0.

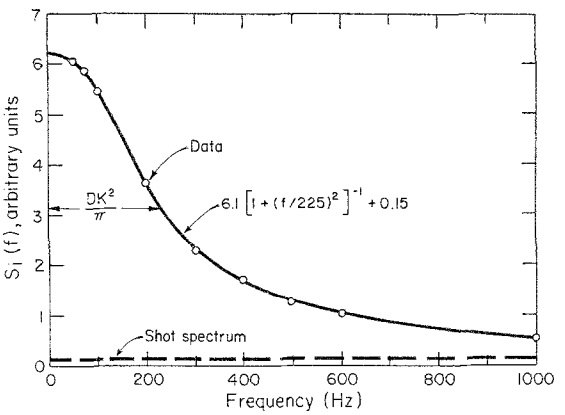

FIG. 3. Photocurrent power spectrum for a suspension of polystyrene spheres of diameter 0.234 μ at a scattering angle $\Theta=90°$. The dashed line represents the shot noise. Using the Stokes–Einstein relation [Eq. (2)] one obtains $DK^2/\pi=223$ Hz, in good agreement with the experimental points. The spectrum analyzer bandwidth is 10 Hz.

Let us now calculate the correlation function for the scattered electric field and for the intensity of the scattered light, as a comparison of the information contained in each is instructive. From Eq. (6) we see that

$$\begin{aligned} R_E(\tau)&\equiv\langle \mathbf{E}^*(t)\mathbf{E}(t+\tau)\rangle \\ &=|\,E_0'\,|^2\exp(-i\omega_0\tau) \\ &\quad\times\Big\langle\sum_k\sum_j\exp\{-i[\phi_k(t)-\phi_j(t+\tau)]\}\Big\rangle. \end{aligned} \tag{15}$$

If the particles move in such a way that the kth particle motion is uncorrelated with that of the jth particle, only terms for which $k=j$ enter the double sum after ensemble averaging. For $k\neq j$,[9]

$$\begin{aligned} \langle\exp\{-i[\phi_k(t)-\phi_j(t+\tau)]\}\rangle&=\langle\exp[-i\phi_k(t)]\rangle \\ &\quad\times\langle\exp[+i\phi_j(t)]\rangle=0. \end{aligned}$$

Furthermore, since each particle is equivalent to each of the others, the resulting sum over k is N times the ensemble average of the phase factor difference $[\phi(t)-\phi(t+\tau)]$ for a single particle. Thus,

$$\begin{aligned} R_E(\tau)&=N\,|\,E_0'\,|^2\exp(-i\omega_0\tau) \\ &\quad\times\langle\exp\{-i\mathbf{K}\cdot[\mathbf{r}(t)-\mathbf{r}(t+\tau)]\}\rangle \end{aligned} \tag{16}$$

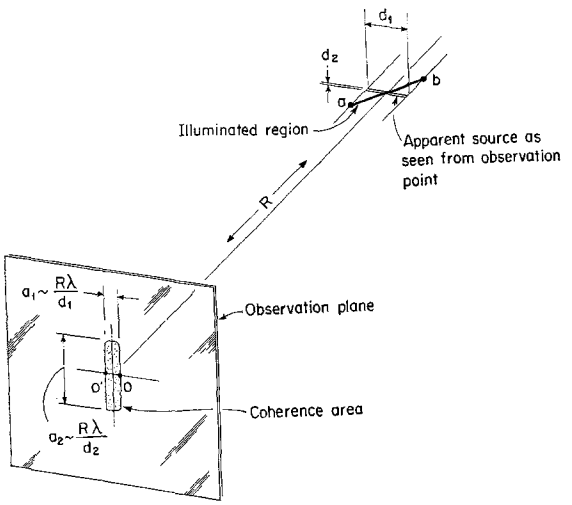

FIG. 4. Typical configuration of an illuminated region and the resulting coherence area. If the observation point is moved from 0 to 0′, the relative phase of the waves scattered from points a and b changes by $\sim\pi$.

where we used

$$\phi(t)=\mathbf{K}\cdot\mathbf{r}(t). \tag{17}$$

This ensemble average represents an integral of $\exp(i\mathbf{K}\cdot\Delta\mathbf{r})$ over the conditional probability distribution $P(\Delta\mathbf{r},\tau\mid 0,0)$ describing the probability that a particle located at position $\mathbf{r}$ at time zero will be found at position $\mathbf{r}+\Delta\mathbf{r}$ at time τ later. Thus since $\mathbf{r}(t+\tau)-\mathbf{r}(t)=\Delta\mathbf{r}$, we have

$$\langle\exp\{-i\mathbf{K}\cdot[\mathbf{r}(t)-\mathbf{r}(t+\tau)]\}\rangle = \int_{-\infty}^{\infty} d^3\Delta\mathbf{r}P(\Delta\mathbf{r},\tau\mid 0,0)\exp(i\mathbf{K}\cdot\Delta\mathbf{r}). \tag{18}$$

The probability distribution $P(\Delta\mathbf{r},\tau\mid 0,0)$ is well known for the random walk problem and is given by Eq. (1). On substituting from Eq. (1) into Eq. (18) we find at once that

$$R_E(\tau)=N\mid E_0'\mid^2\exp(-i\omega_0\tau-DK^2\mid\tau\mid). \tag{19}$$

It is possible to understand simply why the correlation function for the scattered field falls to zero when τ substantially exceeds the correlation time $\tau_c=1/DK^2$. Any superposition of the phases of the scattered waves will change to a new uncorrelated superposition of phases after the elapse of sufficient time so that the phase of each particle has changed by $\sim\pi$. In order to change phase by π the particle must move a distance π/K along the direction of K. In the case of three-dimensional random walk, however, the mean square distance moved in time t in a particular direction (call it the X direction) is given by[6]

$$\langle\Delta X^2\rangle=6Dt. \tag{20}$$

If this mean square distance is chosen to be $(\pi/K)^2$, we see that the time required for a loss of correlation in the superposition of scattered phases is

$$\tau_c\sim(\tfrac{1}{6}\pi^2)(1/DK^2), \tag{21}$$

which is consistent with the rigorous result as expressed in the correlation function in Eq. (19).

The quantity DK^2 measures the spectral width of the scattered light. This is seen by calculating the spectrum of the light using Eqs. (19) and (13). This gives

$$S_E(\omega)=2N\mid E_0'\mid^2\{DK^2/[(\omega-\omega_0)^2+(DK^2)]^2\}. \tag{22}$$

Thus the spectrum of the scattered light is a Lorentzian shaped line centered around the incident light frequency. Its half-width at half-height $(\Delta f)_{1/2}$ is

$$(\Delta f)_{1/2}=DK^2/2\pi. \tag{23}$$

A numerical calculation for the spectral width for scattering angle $\Theta=90°$, $\lambda=6328$ Å, and spheres of radius $a=630$ Å in water gives $DK^2/2\pi=200$ Hz.

Let us now calculate the correlation function for the intensity fluctuations. Using Eq. (6) and $I(t)=\beta\mid\mathbf{E}(t)\mid^2$, we see that

$$R_I(\tau)=\langle I(t)I(t+\tau)\rangle=\beta^2\langle\mid\mathbf{E}(t)\mid^2\mid\mathbf{E}(t+\tau)\mid^2\rangle \tag{24}$$

or

$$R_I(\tau)=\mid E_0'\mid^4\beta^2\times\Big\langle\sum_m\sum_j\sum_k\sum_l\exp\{i[\phi_m(t)-\phi_j(t)]\}\times\exp\{i[\phi_k(t+\tau)-\phi_l(t+\tau)]\}\Big\rangle. \tag{25}$$

The statistical independence of the particle positions insures that any term with indices $mjkl$ will be zero if one index is different from the other three. Thus, only terms in which the indices $mjkl$ contain at least pairs of equal indices are nonzero.[9] There are N^2 terms for which $m=j$ and $k=l$, each of which is equal to unity. We also have (N^2-N) terms for which $m=l$ and $j=k$, but $m\neq j$. Each

such term has the form

$$\langle \exp\{i[\phi_1(t)-\phi_1(t+\tau)]\} \times \exp\{-i[\phi_2(t)-\phi_2(t+\tau)]\}\rangle. \quad (26)$$

Finally we have terms for which $m=k$ and $j=l$, but $m\neq j$, and these give zero on ensemble averaging over the starting phases. Hence, if we neglect N compared to N^2 we seen that the intensity correlation function is given by

$$R_I(\tau)=N^2\,|\,E_0'\,|^4\beta^2 \times(1+\langle \exp\{i[\phi_1(t)-\phi_1(t+\tau)]\} \times \exp\{-i[\phi_2(t)-\phi_2(t+\tau)]\}\rangle). \quad (27)$$

Since each particle is independent of the others, we may write this in the equivalent form

$$R_I(\tau)=N_2\,|\,E_0'\,|^4\beta^2 \times(1+\,|\langle \exp\{-i[\phi(t)-\phi(t+\tau)]\}\rangle|^2). \quad (28)$$

Thus the correlation function for the intensity fluctuation consists of a τ independent part corresponding to the time-averaged part of the intensity, and a second part which is essentially the square of the correlation function for the electric field. The oscillating part $[\exp(i\omega_0\tau)]$ of the field correlation function disappears in the intensity correlation function because the intensity depends only on the field amplitude. Using the fact that

$$\langle \exp\{-i[\phi(t)-\phi(t+\tau)]\}\rangle=\langle \exp[i\mathbf{K}\cdot\Delta\mathbf{r}(\tau)]\rangle = \exp(-DK^2\,|\,\tau\,|), \quad (29)$$

as we saw on obtaining Eq. (19), we find that

$$R_I(\tau)=N^2\,|\,E_0'\,|^4\beta^2[1+\exp(-2DK^2)|\,\tau\,|]. \quad (30)$$

The spectrum of the intensity fluctuations can be obtained using Eqs. (30) and (14), and the symmetry of $R_I(\tau)$ around $\tau=0$. Thus,

$$S_I(\omega)=N^2\,|\,E_0'\,|^4\beta^2(2\pi\delta(\omega) +\{2(2DK^2)/[\omega^2+(2DK^2)^2]\}). \quad (31)$$

We observe at once that the spectrum of the intensity fluctuations (apart from the dc component centered at $\omega=0$) consists of a Lorentzian line whose center is at zero frequency and whose width is twice the width of the spectrum for the electric field. Since the intensity fluctuation spectrum, or the spectrum of the photocurrent, is located around dc where narrow electrical filters are available, one can easily measure the photocurrent spectrum even if it is a few Hertz wide. A measurement of this photocurrent spectral width provides the diffusion constant in accordance with the relation

$$(\Delta f)_{1/2}=DK^2/\pi. \quad (32)$$

Here $(\Delta f)_{1/2}$ is the half-width at half-height of the spectrum of the intensity fluctuations. In effect the squaring action of the photocathode shifts the optical information downwards in frequency from its original value at the optical frequency ($\sim 10^{14}$ cps) to a value centered at dc where one can conveniently analyze the spectral shape and width. This method of spectroscopy is the analog, in the optical-frequency regime, of the well-known crystal set used to receive radio signals. In the radio-wave case, the information is also contained in a narrow range of signal frequencies centered around a high carrier frequency. The crystal is a square-law device which removes the high-frequency carrier and passes the signal frequencies centered now near dc.

III. SPECTRUM OF THE PHOTOCURRENT AND THE SIGNAL-TO-NOISE RATIO

We now proceed to obtain the correlation function and the spectrum of the photocurrent when the PMT is illuminated by the scattered light. Since it will be shown in Sec. IV that the intensity fluctuations are spatially correlated over only a certain area called the coherence area A_c, let us assume that the photosurface is illuminated over just this area A_c. The rate of emission of photoelectrons $[\dot{n}(t)]$ from the photocathode is proportional to the rate of arrival of photons in this area, i.e., $\dot{n}(t)=(\eta A_c/\hbar\omega)I(t)\equiv\alpha I(t)$, where η is the quantum efficiency and $\hbar\omega$ is the photon energy. Each photoelectron produces at the anode a photopulse of duration $\sim 10^{-9}$ sec which carries a charge Ge, where G is the gain of the photomultiplier and e is the electronic charge. The average photocurrent $\langle i\rangle$ is thus

$$\langle i\rangle=Ge\langle\dot{n}\rangle=Ge\alpha\langle I\rangle. \quad (33)$$

The correlation function for the temporal fluctuations of the photocurrent contains two parts. The first describes the temporal correlation in the

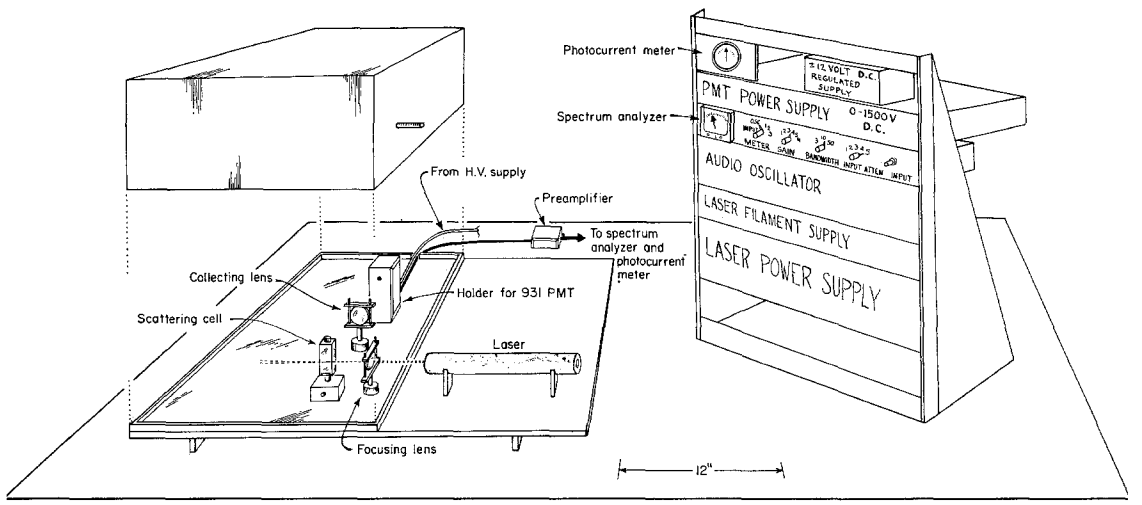

FIG. 5. Drawing of the experimental apparatus.

fluctuations of the light intensity $I(t)$. The second, the shot part, describes the fact that the photocurrent is made up of pulses. Both these effects lead to the following form for the photocurrent correlation function[8,10]:

$$R_i(\tau) = \langle i(t)i(t+\tau)\rangle = \langle i\rangle^2[R_I(\tau)/\langle I\rangle^2] + Ge\langle i\rangle p(\tau). \quad (34)$$

Here $p(\tau)$ is the correlation function for a photopulse. It is generally very much narrower than $R_I(\tau)$. In fact $p(\tau)\sim 0$ for $|\tau| > 10^{-9}$ sec. Its integral over τ is unity. Thus for all frequencies below $\sim 5\times 10^8$ cps we may replace $p(\tau)$ by $\delta(\tau)$, the Dirac delta function. The spectrum of the photocurrent is obtained by using the Wiener–Khintchine theorem. Carrying out this Fourier transformation using Eq. (30) for $R_I(\tau)$ and Eq. (31) for its Fourier transform, along with the fact that $\langle I\rangle^2 = N\,|\,E_0'\,|^2\beta$, we find

$$S_i(\omega) = \langle i\rangle^2(2\pi\delta(\omega) + \{2(2DK^2)/[\omega^2 + (2DK^2)^2]\}) + Ge\langle i\rangle. \quad (35)$$

The spectrum of the photocurrent contains: a dc component $[2\pi\delta(\omega)]$, the intensity fluctuation spectrum, and a frequency-independent "white" noise spectrum produced by the "shot" or pulselike nature of the photocurrent. In general the frequency response of the amplifiers in the spectrum analyzer are not entirely independent of frequency. This can produce an apparent slow frequency dependence in the shot part of the spectrum. This effect can be measured and corrected for by measuring the photocurrent spectrum while the photomultiplier is illuminated with constant intensity light as discussed in Sec. V.

We may form a preliminary estimate of the strength of the intensity fluctuation spectrum by comparing it, the signal, with the shot part of the spectrum. Putting aside the dc contribution of the light to the photocurrent spectrum, and designating as $(S/N)_{\text{pre}}$, the ratio of the signal spectral power density at $\omega = 0$ to the shot spectral power density, we find, using the notation $1/\tau_c = DK^2$, that

$$(S/N)_{\text{pre}} = \langle i\rangle^2\tau_c/Ge\langle i\rangle = \langle \dot{n}\rangle\tau_c. \quad (36)$$

Equation (36) indicates that the signal power spectral density is comparable with the shot power spectral density when at least one photopulse is produced by the light in one coherence area during one correlation time τ_c. Here τ_c is the correlation time for the fluctuation in the electric field. This relationship was first obtained by Forrester[11] and studied by Bergé *et al.*[12]

The ratio given in Eq. (36) is, in itself, not a useful measure of the detectibility of the signal. Uncertainty in the detectibility of the signal is a result of fluctuations in the output of the spectrum analyzer which records the spectrum of the photocurrent. These fluctuations arise because the measurement of the power spectral density is made in a finite time. The power spectral density computed in the Wiener–Khintchine theorem is that which would be obtained if the measurements were

made with an infinite final averaging time. Experimentally the spectrum analyzers have two filters: a predetection filter of width $(\Delta f)_{\text{pre}}$, and a final time averaging filter of width $(\Delta f)_{\text{post}}$. The frequency width of the latter is the reciprocal of the averaging time used to determine the mean power passing through the predetection filter. As we shall show in the Appendix, the mean-square fluctuation in the output meter reading of the spectrum of the photocurrent, is given by

$$(\text{noise})^2 = S_i^2(f)\,(\Delta f)_{\text{post}}(\Delta f)_{\text{pre}}, \qquad (37)$$

where $f=\omega/2\pi$. The measure of the detectibility of the signal which we shall use is the ratio of the power in the signal (near $f=0$) to the rms fluctuation in the spectrum analyzer output. Calling this the signal-to-noise ratio, we have

$$\frac{S}{N} = \frac{S_i(0)_{\text{sig}}\Delta f_{\text{pre}}}{[(S_i(0))_{\text{sig}}+(S_i(0))_{\text{shot}}](\Delta f_{\text{post}}\Delta f_{\text{pre}})^{1/2}}, \qquad (38)$$

$$\frac{S}{N} = \frac{(S/N)_{\text{pre}}}{(1+(S/N)_{\text{pre}})}\cdot\left(\frac{\Delta f_{\text{pre}}}{\Delta f_{\text{post}}}\right)^{1/2}. \qquad (39)$$

Since $\Delta f_{\text{post}} \sim I/T$, where T is the time of measurement, the signal-to-noise ratio is proportional to the square root of this measuring time. When the predetection-signal-to-noise ratio is small compared to unity, the ratio $(S/N)_{\text{pre}}$ is a most important factor in increasing the detectibility of the signal. If, however, $(S/N)_{\text{pre}}$ is much greater than unity, the signal-to-noise ratio is completely independent of the predetection-signal-to-noise ratio and depends only on the ratio of the post and predetection bandwidths.[4] This limit is often encountered in the study of light scattered from large macromolecules or latex spheres [$(S/N)_{\text{pre}} \sim 40$ for the data of Fig. 3.]

As a final point we may consider how the photocurrent spectrum and the signal-to-noise ratio would be altered if say m different areas of coherence fall on the surface of the phototube. In such a case the dc term of the photocurrent spectrum is multiplied by m^2, and the shot term is multiplied by m. The signal part is also multiplied by m since the fluctuations between coherence areas are uncorrelated. Thus, since both the signal and shot parts of the spectrum are linearly proportional to m there is no change in either the predetection-signal-to-noise or the postdetection-signal-to-noise ratio over that which we obtained above for a single coherence area.

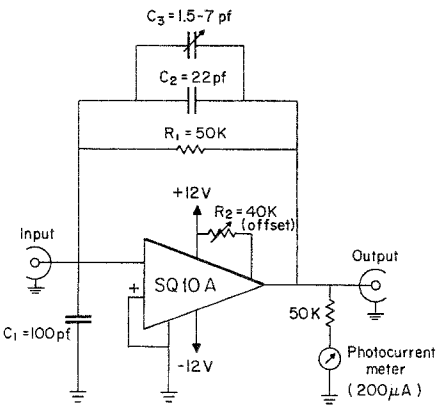

FIG. 6. Low input independence preamplifier. Trim R_2 for zero offset; C_3 for flat response with the photomultiplier used.

IV. DEMONSTRATION

The qualitative features of these intensity fluctuations are observable in a demonstration that requires only a laser, a lens, the sample, and a white card, arranged as in Fig. 1. For large spheres (diameter $\sim 1\,\mu$) in sufficient concentration, a pattern of bright twinkling spots, continually in motion, appears about the direct beam from the laser. Inspection of the spots shows that (a) the coherence area, i.e., the area, at a fixed time, over which the intensity does not change appreciably (the average spot size) increases for smaller scattering angles; and (b) the time variation of the intensity over a coherence area becomes slower for smaller scattering angles.

The first effect (a), which has been investigated by Bergé and Volochine,[13] results from the fact that at a fixed time the optical path from a given particle to the observation point changes relative to that of the other particles as the observation point is moved, introducing changes in the phase relations of the scattered waves. As the observation point is moved the intensity will remain nearly constant as long as the relative phase changes are small ($\ll\pi$). Referring to Fig. 4, for a source of apparent dimension d_1 along some direction, this condition will be satisfied for observation points separated in that direction by a distance $a_1 < \lambda R/d_1$, $\lambda R/d_1$ being the translation of the observation point necessary to produce a relative phase change of $\sim\pi$ for particles at the

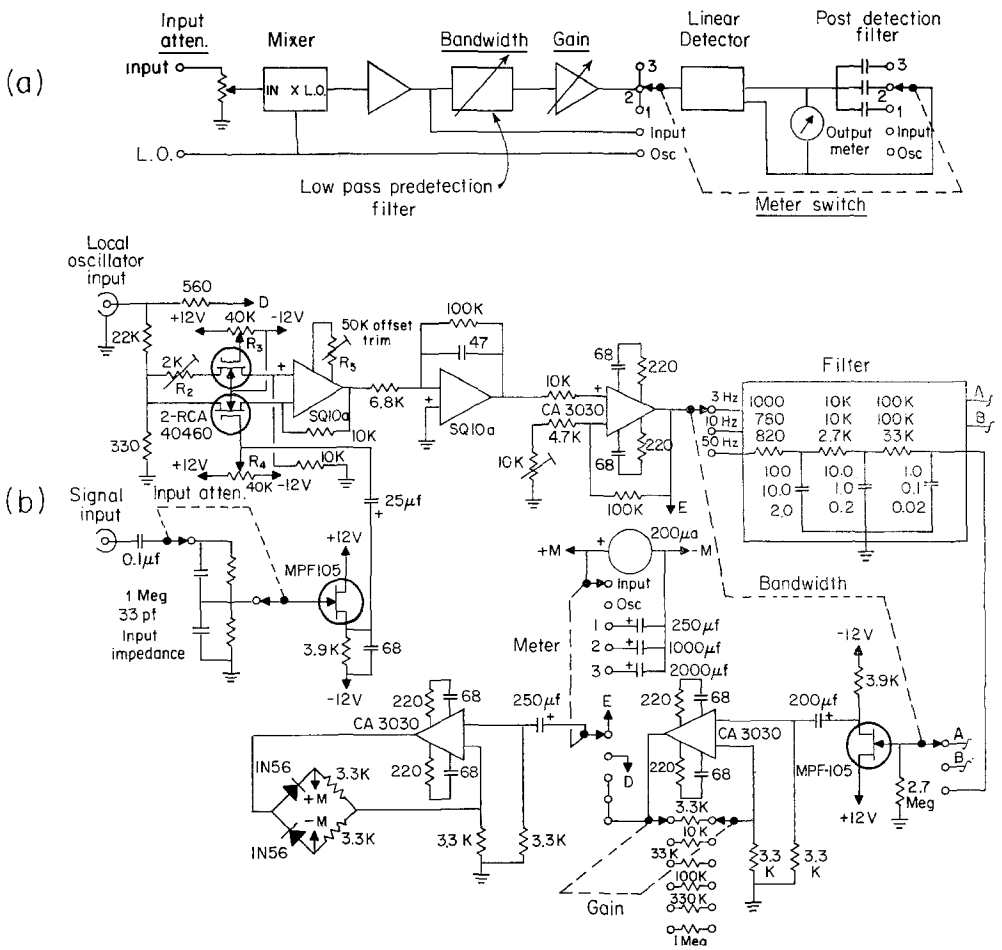

FIG. 7. (a) Block diagram of spectrum analyzer. (b) Schematic diagram of spectrum analyzer. Adjust R_2 for minimum carrier leakage. Adjust R_3, R_4, and R_5 for minimum distortion at input to filter with 1-V rms at local oscillator input and 0.5 V p–p square wave at signal input. Resistance values are in ohms, capacitance values in pF, except in the filter where capacitance values are in μF. If unavailable, the RCA 40460 may be replaced by RCA 3N138 or 3N153.

extremities of the source. The apparent length (d_1) of the illuminated region decreases with scattering angle as one approaches the forward direction and this results in the increase in size of the spots.

The second effect (b) is a direct manifestation of the dependence of the correlation time $\tau_c = 1/DK^2$ on the scattering angle. According to Eq. (11) and our discussion following Eq. (19), we see that the correlation time increases as the reciprocal of $\sin^2\frac{1}{2}\Theta$, where Θ is the scattering angle. This is because for the smaller scattering angles the diffusing particles must move a longer distance before they lose their phase relations relative to one another. The characteristic twinkling time is just the correlation time for the intensity fluctuation and this varies as $1/DK^2$, where $K = (4\pi/\lambda)\sin\frac{1}{2}\Theta$. The slowing down is a direct measure of the K^2 dependence for the correlation rate.

With a 1-mW helium–neon laser and 1-μ-diam spheres, this demonstration may be shown in a reasonably dark room to a small number of students. With a higher-power laser, the card may be moved further from the scattering cell and shown to a larger group.

V. EXPERIMENT

The laboratory experiment consists of physically realizing the various components illustrated in Fig. 1 and described in our theoretical analysis. It enables one to measure the photocurrent spec-

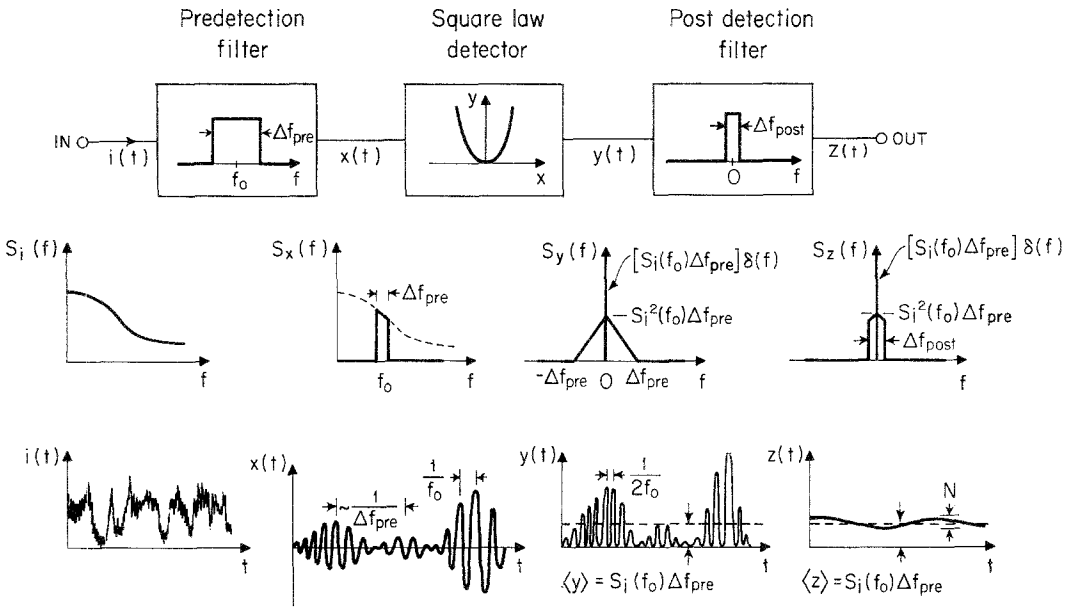

FIG. 8. Model spectrum analyzer showing the effect of the primary components.

trum $S_i(\omega)$, and to determine the half-width at half-height and the shape of the signal part of the photocurrent spectrum as shown in Fig. 3. The spectrum is obtained by passing the fluctuating photocurrent through an audio spectrum analyzer. This spectrum analyzer is simply a tunable predetection filter of passband Δf_{pre} followed by a linear detector and a final time averaging filter of passband $\Delta f_{\text{post}} = I/T$. The square of the dc output of the final filter, when the spectrum analyzer is set at a frequency f, is proportional to the average ac power in the photocurrent around f within the band pass of the predetection filter [thus proportional to $S_i(f) \cdot \Delta f_{\text{pre}}$]. A drawing of the experimental apparatus is shown in Fig. 5.

The following apparatus is needed for the experiment.

(a) Laser. A helium–neon laser providing 1 mW or more is required. It must be free of audio frequency amplitude modulation, including 60 and 120 Hz. This is sometimes produced by ac filament currents or unregulated discharge supplies. The suitability of a laser should be checked by allowing a small portion of the output beam to fall on the photosurface, and then measuring the intensity fluctuation spectrum of the laser itself. This should be frequency independent.

(b) Sample. Samples are prepared by diluting the concentrated suspensions with distilled water, free from large particles. Concentrated aqueous suspensions of monodisperse polystyrene spheres are available from the Dow Chemical Co., Diagnostic Products Dept., Indianapolis, Ind. Filters available from the Millipore Corp. (Bedford, Mass.) are convenient for cleaning the solvent although this is generally not necessary at the high concentrations used here. The samples are held in glass photometric cells available from Lux Scientific Instrument Co. (Canal St. Station, New York, N.Y.).

(c) Photomultiplier. Any photomultiplier will do, the higher the gain the better. The RCA 931 was chosen because of easy availability and low cost. A variable, ripple-free, dc high-voltage supply (500–1500 V) is required for the PMT. Its voltage must be variable so that the dc photocurrent level can be adjusted.

(d) Preamplifier. Care must be taken to avoid excessive shunt capacitance across the PMT load resistor because this will roll off the PMT response at high frequencies in the audio range. This problem is avoided if the PMT drives a low impedance load. The preamplifier circuit (see Fig. 6) provides a flat response to 50 KHz and costs about $25 to construct.

(e) Spectrum analyzer. Any audio frequency spectrum analyzer of bandwidth 3–50 Hz and an operating range of 10 Hz–20 KHz will do. Because

these instruments are generally expensive, we have designed (see Fig. 7) circuits suitable for an advanced laboratory experiment which can be built for less than $200, not counting the cost of a variable frequency, low distortion audio oscillator and a ±12-V regulated dc power supply. A block diagram of the spectrum analyzer is shown in Fig. 7(a). First, the input signal is multiplied by the local oscillator signal in the mixer. Frequency components in the input signal near the local oscillator frequency appear near dc at the output of the mixer. The signal is then filtered by a low-pass predetection filter, amplified, and detected by a full wave "linear" detector. Since the output fluctuations depend upon the filter bandwidth, the detector output (postdetection) time constant is adjustable to provide for easier meter reading (data are taken by averaging many independent meter readings). To avoid at the output of the mixer the appearance of frequency components of the input signal near harmonics of the local oscillator frequency, it is essential that a low-distortion local oscillator be used and that the mixer output be accurately the product of the input signal and the local oscillator signal. To achieve this we have used an analog multiplier circuit[14] that gives the desired product to about 0.1%.

The equipment is set up as shown in Fig. 1 with the incident polarization normal to the scattering plane. The concentration should be adjusted as high as possible, while keeping the laser beam in the sample more intense than the halo about the beam produced by rescattering of scattered light. Due to the angular acceptance of the collection optics and the angular divergence of the focused incident beam, scattered light with a distribution of scattering angles over some range $\Delta\Theta$ will be collected by the PMT. The measured spectrum then is a superposition of Lorentzians with a distribution of half-widths. It can be shown, however, that for even with rather broad distributions of half-widths the observed spectrum will be a Lorentzian to a high degree of accuracy.[15] Since according to Eq. (5) the linewidth $\Gamma(\Theta)$ is a nonlinear function of Θ, the average observed linewidth may not be that corresponding to the average scattering angle, especially in the forward direction where $\Gamma \propto \Theta^2$. However, by choosing $\Delta\Theta$ such that $\Delta\Gamma/\Gamma < 0.1$ these effects can be made negligible. Differentiating Eq. (5) we find that for $\Delta\Gamma/\Gamma < 0.1$, $\Delta\Theta < 0.1 \tan\frac{1}{2}\Theta$. Thus for $\Theta = 90°$, $\Delta\Theta < 0.1$ rad $= 5°$. To produce large areas of spatial coherence in the scattered field (thereby increasing the scattered power per coherence area and thus the predetection-signal-to-noise ratio according to the remarks of Sec. III) the beam should be focused in the cell. We note here that $\mathbf{k}_0$ in the derivation is that in the scattering medium and must be calculated using the index of refraction (n) of the sample $(\mathbf{k}_0)_{\text{sample}} = n(\mathbf{k}_0)_{\text{vac}}$. Also, the refraction of the scattered light at the cell wall must be accounted for when determining the scattering angle.

The frequency response of the electronic system may be determined by measuring the spectrum of the shot noise, obtained by illuminating the PMT with constant-intensity light. A flashlight lamp powered by a stable battery source serves well here. To obtain the largest shot noise power one should use a combination of the largest permissible PMT voltage (1500 V for the 931) and the least light intensity which produces the desired photocurrent ($\sim 100\ \mu$A). To measure a fluctuation spectrum, however, a large signal-to-shot ratio $(S/N)_{\text{pre}}$ is desirable. This is accomplished by using the combination of largest scattered intensity and lowest PMT voltage which produces the desired photocurrent. With no input to the spectrum analyzer, the output meter, due to carrier leakage, will read slightly up scale at low frequencies. This must be subtracted from the meter readings of any spectrum measured.

Data analysis proceeds as follows. If the detector on the spectrum analyzer is linear, as in the one above, the output must be squared to obtain the spectrum. To correct the squared output spectrum for the frequency response of the spectrum-analyzer electronics, this spectrum may be divided by the square of the shot spectrum. For a square-law detector the output of the spectrum analyzer directly gives the power spectrum. A spectrum such as Fig. 3 is then obtained. Figure 3 shows the measured photocurrent power spectrum for a suspension of polystyrene spheres of diameter 0.234 μ as a scattering $\Theta = 90°$. The dashed line represents the shot spectrum.

APPENDIX

We demonstrate here in a correct, but qualitative way the validity of Eq. (37) for the mean-square amplitude of the noise fluctuation in the

output meter of a spectrum analyzer.[16,17] In Fig. 8 we indicate the primary components of the spectrum analyzer, and illustrate their effect by plotting spectral power densities and typical voltage at the indicated points.

Suppose that the predetection filter is held fixed at some frequency f_0. The output of this filter will contain all the frequencies between $f_0-\frac{1}{2}\Delta f_{\rm pre}\leq f\leq f_0+\frac{1}{2}\Delta f_{\rm pre}$ that are in the photocurrent fluctuations. The square-law device squares these frequency components and has as its output three characteristic spectral components.

The first is a dc component ($\langle y\rangle$) which has the magnitude $S_i(f_0)\Delta f_{\rm pre}$ and is the spectral power that we wish to determine. The second component consists of frequencies near $2f$ which we shall neglect because they are not passed by the final postdetection filter. The third component consists of "self-beat" notes between all the spectral components in the range $f_0-\frac{1}{2}\Delta f_{\rm pre}\leq f\leq f_0+\frac{1}{2}\Delta f_{\rm pre}$. These notes are distributed in a spectrum which is the convolution of the rectangular predetection filter with itself and produce the amplitude variation of the oscillatory part of $y(t)$. This spectral density has a maximum at zero frequency where it is $S_i^2(f)\Delta f_{\rm pre}$, and it falls linearly to zero at a frequency equal to $\Delta f_{\rm pre}$.

The final filter of width $(\Delta f)_{\rm post}$ transmits all of the dc long-time mean signal, i.e., $S_i(f_0)\Delta_{\rm pre}$. This appears on the meter as $\langle z\rangle$, the signal level. The final filter transmits only frequencies between zero and $(\Delta f)_{\rm post}$ of the self-beat spectrum coming out of the square-law detector. Thus, the mean-square power in these self-beat notes is $[S_i^2(f_0)\Delta f_{\rm post}]\Delta f_{\rm pre}$. This is the mean-square fluctuation in the output of the recording meter: $N^2=S_i^2(f_0)\Delta f_{\rm post}\Delta f_{\rm pre}$. In operation if f is held fixed, the output meter, which can change only in times of the order of $T\sim 1/(\Delta f)_{\rm post}$, will wander back and forth around the signal $S_i(f_0)\Delta f_{\rm pre}$. The total mean-square needle excursion after many periods T is given by the equation above for N^2.

* A brief account of this work has appeared in Amer. J. Phys. **37**, 853 (1969).

† This research was supported in part with funds provided by the Advanced Research Projects Agency under Contract SD-90 with the Massachusetts Institute of Technology.

[1] R. Pecora, J. Chem. Phys. **40**, 1604 (1964).

[2] H. Z. Cummins, N. Knable, and Y. Yeh, Phys. Rev. Letters **12**, 150 (1964).

[3] S. B. Dubin, J. H. Lunacek, and G. B. Benedek, Proc. Natl. Acad. Sci. (U. S.) **57**, 1164 (1967).

[4] G. B. Benedek, in the Jubilee Volume in honor of Alfred Kastler, *Polarization, Matter and Radiation* (Presses Universitaire de France, Paris, 1969), p. 49.

[5] H. Z. Cummins and H. L. Swinney, in *Progress in Optics*, E. Wolf, Ed. (to be published).

[6] C. Kittel, *Elementary Statistical Physics* (John Wiley & Sons, Inc., New York, 1958), p. 156; M. C. Wang and G. Uhlenbeck, Rev. Mod. Phys. **17**, 326 (1945).

[7] A. Einstein, *Investigations on the Theory of Brownian Movement*, R. Furth, Ed. (Dover Publ., Inc., New York, 1956).

[8] W. B. Davenport and W. Root, *An Introduction to the Theory of Random Signals and Noise* (McGraw-Hill Book Co., New York, 1958), Chap. 6; C. Kittel, *Elementary Statistical Physics* (John Wiley & Sons, Inc., New York, 1958), p. 136; F. Reif, *Fundamentals of Statistical and Thermal Physics* (McGraw-Hill Book Co., New York, 1965), p. 585.

[9] This will fail for scattering angles very close to zero, that is, in the extreme forward direction, where $K\cong 0$. However, for scattered light falling outside of the direct beam we will have $Ka>2\pi$, where a is the apparent source dimension as seen from the forward direction. This will assure that $\langle\exp(i\phi_j)\rangle$, $\langle\exp[i(\phi_k+\phi_j)]\rangle=0$.

[10] C. Freed and H. Haus, Phys. Rev. **141**, 287 (1966).

[11] A. T. Forrester, J. Opt. Soc. Amer. **51**, 213 (1961), Eq. (6).

[12] P. Berge, B. Volochine, M. Adam, P. Calmettes, and A. Hamelin, Compt. Rend. **B266**, 1575 (1968).

[13] P. Bergé and B. Volochine, Compt. Rend. **B264**, 1200 (1967).

[14] Siliconix Incorporated, 1440 W. Evelyn Ave., Sunnyvale, Calif., catalog sheet for FET transistor #VCR3P.

[15] S. B. Dubin (private communication).

[16] We consider here a spectrum analyzer with a square-law detector. Similar considerations apply to one with a linear detector as is used in this experiment.

[17] Reference 8, Davenport and Root, Chap. 12.